

Hydrothermal Synthesis and Structure of the Solid Solution $(\text{Fe}_{0.54}\text{Mn}_{0.46})(\text{PO}_4)\cdot 2\text{H}_2\text{O}$

Nadia Belfguira · Siwar Walha · Ahlem Kabadou ·
Abdelhamid Ben Salah · Frédéric Hatert ·
André Mathieu Fransolet

Received: 14 January 2010/Accepted: 3 September 2010/Published online: 15 September 2010
© Springer Science+Business Media, LLC 2010

Abstract The iron-manganese phosphate of composition $(\text{Fe}_{0.54}\text{Mn}_{0.46})(\text{PO}_4)\cdot 2\text{H}_2\text{O}$ has been obtained as a single-phase product using hydrothermal methods and the structure has been determined by single crystal X-ray diffraction. The title compound is orthorhombic, Pbca, $a = 8.720(1)$, $b = 9.884(1)$, $c = 10.114(2)$ Å, isostructural with strengite. The structure consists of a linkage of MO_6 octahedra and PO_4^{3-} tetrahedra. The octahedra are insular and are held together to form a three-dimensional structure by the tetrahedra. The crystal structure study revealed that $(\text{Fe}_{0.54}\text{Mn}_{0.46})(\text{PO}_4)\cdot 2\text{H}_2\text{O}$ exhibits a strong Jahn–Teller effect. The compound has been characterized by Raman and IR Spectroscopy, showing the bonds characteristic of the PO_4^{3-} polyanions. Measurements by the electric permittivity revealed a peak at 350 K.

Keywords Iron phosphate · Manganese phosphate · Hydrothermal synthesis

Introduction

Transition metal phosphates have been extensively investigated due to their structural variability. Many of these materials are studied for their use as catalysts [1], ion exchangers [2], dielectric [3], electric [4], and magnetic [5] properties.

N. Belfguira (✉) · S. Walha · A. Kabadou · A. B. Salah
Laboratoire des Sciences des Matériaux et d'environnement,
Faculté des Sciences de Sfax, BP 1171, 3000 Sfax, Tunisia
e-mail: n.belfguira@yahoo.fr

N. Belfguira · F. Hatert · A. M. Fransolet
Laboratoire de Minéralogie, Département de Géologie,
Bâtiment B18, Université de Liège, 4000 Sart-Tilman, Belgium

Hydrothermal techniques provide an intimate mixing of the component elements in the solution, allowing finer particles and high purity materials to be produced by rapid homogenous nucleation. Manganese phosphates and manganese phosphate hydrates have been synthesized either by hydrothermal or by high-temperature methods and are also found in nature. Up to now the following Mn(III)-compounds have been found and characterized by single-crystal structure determination or from microcrystalline powders: $\text{MnPO}_4 \cdot \text{H}_2\text{O}$ [6], $\text{Mn}(\text{PO}_4)_2 \cdot 0.962 \text{D}_2\text{O} \cdot 0.038\text{H}_2\text{O}$ [7], $(\text{Fe}^{3+}, \text{Mn}^{3+})\text{PO}_4$ [8], MnHP_2O_7 [9]. Members of the solid-solution series triphylite-lithiophilite $\text{Li}(\text{Fe}^{2+}, \text{Mn}^{2+})\text{PO}_4$, undergo alteration, generally first with oxidation of Fe^{2+} to Fe^{3+} and then of Mn^{2+} to Mn^{3+} , with simultaneous leaching of Li to maintain charge balance. The minerals produced in this step are ferrisicklerite-sicklerite, $\text{Li}_{1-x}(\text{Fe}^{3+}, \text{Mn}^{2+})_x\text{PO}_4$ and heterosite-purpurite $(\text{Fe}^{3+}, \text{Mn}^{3+})\text{PO}_4$. Two crystalline forms of $\text{FePO}_4 \cdot 2\text{H}_2\text{O}$ have been reported in the literature. The metastrengite (phosphosiderite) and strengite forms of $\text{FePO}_4 \cdot 2\text{H}_2\text{O}$ are isostructural with the aluminium phosphates metavariscite and variscite, respectively [10, 11]. They are a common product of hydrothermally reworked triphylite occurring in Li–Fe phosphate bearing pegmatites.

In recent years, much effort has been concentrated on trying to increase the electron transport at the surface of the mostly insulating LiFePO_4 particles [12, 13]. Since the pioneering work of Padhi et al. 1997 [14], mixed orthophosphates LiMPO_4 ($\text{M} = \text{Fe, Co, Ni, Mn}$) isostructural with olivine have been intensively studied as lithium insertion compounds for Li batteries combined with discharge voltage between 3.4 and 4.8 V versus Li/Li^+ . LiFePO_4 leads to high specific energy 150 mAhg⁻¹ [15]. The generation of an appropriately high voltage is due to the presence of the polyanion $(\text{PO}_4)^{3-}$ with strong P–O

covalency, which stabilizes the antibonding $\text{Fe}^{2+}/\text{Fe}^{3+}$, $\text{Mn}^{2+}/\text{Mn}^{3+}$ state through an Fe–O–P and Mn–O–P inductive effect. The synthesis of an iron-manganese phosphate ($\text{Fe}_{0.54}\text{Mn}_{0.46})(\text{PO}_4)\cdot 2\text{H}_2\text{O}$ is reported in this work and the structure study is described.

Experimental

The title compound was prepared from a reaction mixture of H_3PO_4 (4 mmol), FeO (5 mmol) and MnO (5 mmol) in approximately 10 mL of water. The starting mixture was transferred to and sealed in a 23-mL-capacity PTFE-lined stainless steel Parr autoclave under autogenous pressure, filled to approximately 25% volume capacity, and all reactants were stirred briefly before heating. The reaction mixture was heated at 200 °C for 3 days to yield ($\text{Fe}_{0.54}\text{Mn}_{0.46})(\text{PO}_4)\cdot 2\text{H}_2\text{O}$, followed by slow cooling to room temperature. The resulting product was filtered off, washed with deionized water, and dried in air.

A needle-shaped single crystal of ($\text{Fe}_{0.54}\text{Mn}_{0.46})(\text{PO}_4)\cdot 2\text{H}_2\text{O}$ with dimensions given in Table 1 was selected under a polarizing microscope. Diffraction data were collected at room temperature on a Siemens Smart-CCD diffractometer using graphite-monochromated $\text{MoK}\alpha$ radiation. Details of crystal data, intensity collection, and some features of the structure refinement are reported in Table 1. Corrections for Lorentz and polarization effects were done and also for absorption with the empirical ψ scan method [16]. The structures were solved by Patterson methods using the program SHELXS97 (Sheldrick 1997) [17] in the Pbca space group, which allowed determination of the positions of iron and phosphorus atoms. The refinement of the crystal structure was performed by full matrix least-squares based on F^2 using the SHELXL97 program (Sheldrick 1997) [18], allowing determination of the oxygen atomic positions. In the refinement, the occupancy of the Mn site exhibited a significant deviation from full occupancy, indicating a substitution with the Fe atom. Standard SUMP restraints were used for the dimensions of the disordered cations. The x , y , z , and U_{ij} of Fe and Mn atoms have been equated using the EXYZ and EADP restraints, respectively. Final refinement lead to 53 and 47% occupancies, respectively, for the Fe and Mn atoms. The final R -factor is given in Table 1 together with the maximum and minimum peaks in the final Fourier difference synthesis and the goodness of fit. Anisotropic thermal parameters were assigned to all non-hydrogen atoms. The positions of all hydrogen atoms were located from a difference electron-density map and were refined with an O–H bond-length restraint of 0.95(5) Å and with $U_{iso}(\text{H})$ fixed at a value of 0.05 Å². The final atomic positional parameters of ($\text{Fe}_{0.54}\text{Mn}_{0.46})(\text{PO}_4)\cdot 2\text{H}_2\text{O}$ are listed in Table 2. The bond distances and angles of

Table 1 Crystal data and structure refinement for ($\text{Fe}_{0.54}\text{Mn}_{0.46})(\text{PO}_4)\cdot 2\text{H}_2\text{O}$

Formula	$(\text{Fe}_{0.54}\text{Mn}_{0.46})(\text{PO}_4)\cdot 2\text{H}_2\text{O}$
Formula weight (g mol ⁻¹)	186.42
Crystal system	Orthorhombic
Space group	Pbca
a (Å)	8.720(1)
b (Å)	9.884(1)
c (Å)	10.114(2)
Volume (Å ³)	871.76(3)
Z	8
ρ_{calc} (Mg m ⁻³)	2.841
$F(000)$	740
<i>Data collection</i>	
Temperature (K)	293(2)
μ (mm ⁻¹)	3.557
Radiation; λ (Å)	($\text{MoK}\alpha$); 0.71073
Crystal size mm	0.2 × 0.15 × 0.1
Range θ (°)	3.71–31.55
Interval h , k , l	$h \pm 12$, $-13 \leq k \leq 14$, 1 ± 14
No. of measured reflections	12,140
No. of independent reflections	1466
$R(\text{int})$	0.056
<i>Refinement</i>	
Data/restraints/parameters	1466/4/76
R factors [$I > 2\sigma(I)$]	$R_1 = 0.0279$ $wR_2 = 0.0588$
R factors [all data]	$R_1 = 0.0402$ $wR_2 = 0.0638$
Max. and Min. of electronic	0.541, -0.524
Residual density (e Å ⁻³)	
G. O. F	1.000

($\text{Fe}_{0.54}\text{Mn}_{0.46})(\text{PO}_4)\cdot 2\text{H}_2\text{O}$ are given in Table 3. The structure drawings were made using the DIAMOND (Brandenburg and Berndt, 1999) program.

Results and Discussion

The structure consists of linkage of MO_6 octahedra and PO_4^{3-} tetrahedra sharing corners to form a three-dimensional framework. This structure is isostructural with strengite and amounts to a slight orthorhombic distortion of the monoclinic phosphoderite framework.

Each M octahedron shares corners with four P tetrahedra, and the remaining two corners are occupied by two water molecules. Each PO_4 tetrahedron, in its turn, shares four corners with four octahedra. All water molecules in this structure are bonded to the transition metals and thus behave as ligand groups. Because there are no “zeolitic”

Table 2 Atomic coordinates and equivalent isotropic displacement parameters (\AA^2) for $(\text{Fe}_{0.54}\text{Mn}_{0.46})(\text{PO}_4)\cdot 2\text{H}_2\text{O}$. $U(\text{eq})$ is defined as one-third of the trace of the orthogonalized U_{ij} tensor

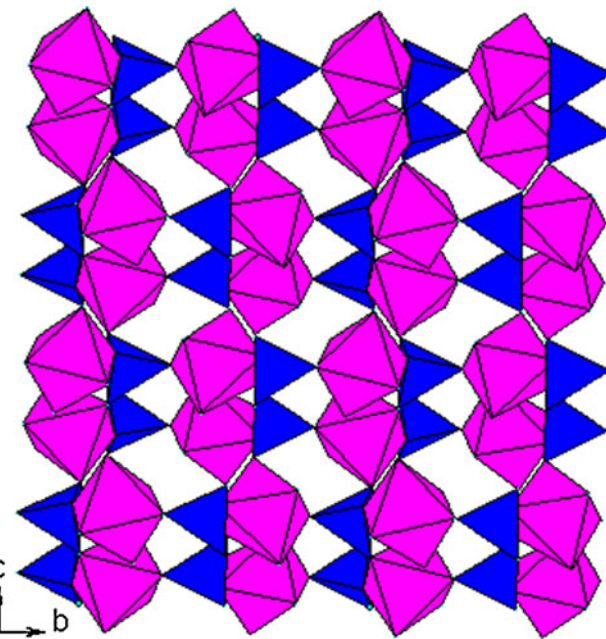
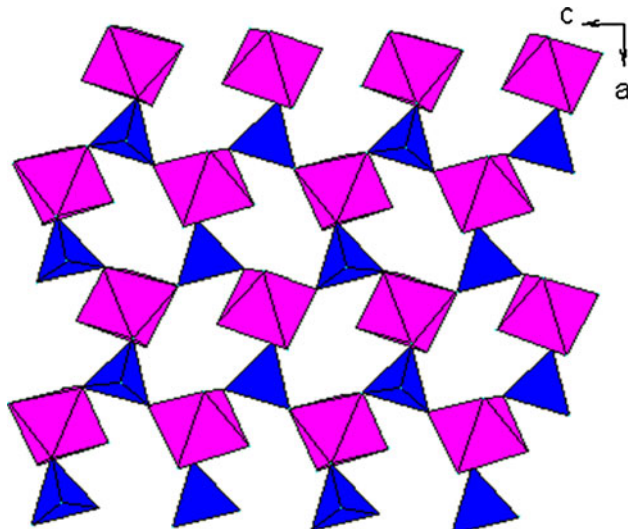
	sof	x/a	y/b	z/c	$U(\text{eq})$
Mn(1)	0.458(1)	0.6516(1)	0.6708(1)	0.8672(1)	0.008(1)
Fe(1)	0.537(1)	0.6516(1)	0.6708(1)	0.8672(1)	0.008(1)
P(1)	1	0.4681(1)	0.8545(1)	0.6484(1)	0.008(1)
O(1)	1	0.3016(2)	0.8202(2)	0.6111(2)	0.013(1)
O(2)	1	0.4843(2)	1.0092(2)	0.6489(2)	0.012(1)
O(3)	1	0.5802(2)	0.7938(2)	0.5472(2)	0.013(1)
O(4)	1	0.5068(2)	0.7950(2)	0.7842(2)	0.013(1)
OW1	1	0.8345(2)	0.5535(2)	0.9398(2)	0.019(1)
OW2	1	0.7351(2)	0.6110(2)	0.6874(2)	0.015(1)

Table 3 Selected bond lengths (\AA) and angles ($^\circ$) for $(\text{Fe}_{0.54}\text{Mn}_{0.46})(\text{PO}_4)\cdot 2\text{H}_2\text{O}$

Mn1–O4	1.951(2)	Mn1–OW1	2.104(2)
Mn1–O3 ⁱ	1.956(2)	P1–O4	1.532(2)
Mn1–O1 ⁱⁱ	1.985(2)	P1–O2	1.536(2)
Mn1–O2 ⁱⁱⁱ	1.995(2)	P1–O3	1.536 (2)
Mn1–OW2	2.046(2)	P1–O1	1.538 (1)
O4–Mn1–O3 ⁱ	94.71(7)	OW2–Mn1–OW1	83.21(7)
O4–Mn1–O1 ⁱⁱ	90.36(7)	O4–P1–O2	111.03(9)
O3 ⁱ –Mn1–O1 ⁱⁱ	88.50(7)	O4–P1–O3	107.90(9)
O4–Mn1–O2 ⁱⁱⁱ	94.81(7)	O2–P1–O3	109.40(9)
O3 ⁱ –Mn1–O2 ⁱⁱⁱ	91.71(6)	O4–P1–O1	110.07(9)
O1 ⁱⁱ –Mn1–O2 ⁱⁱⁱ	174.79(6)	O2–P1–O1	107.87(9)
O4–Mn1–OW2	91.68(6)	O3–P1–O1	110.57(9)
O3 ⁱ –Mn1–OW2	172.93(7)	P1–O1–Fe1 ^{iv}	139.40(7)
O1 ⁱⁱ –Mn1–OW2	94.51(7)	P1–O1–Mn1 ^{iv}	139.40(7)
O2 ⁱⁱⁱ –Mn1–OW2	84.71(6)	P1–O2–Fe1 ^v	137.92 (9)
O4–Mn1–OW1	170.94(7)	P1–O2–Mn1 ^v	137.92(9)
O3 ⁱ –Mn1–OW1	90.84(7)	P1–O3–Fe1 ^{vi}	138.82(9)
O1 ⁱⁱ –Mn1–OW1	82.63(6)	P1–O3–Mn1 ^{vi}	138.82(9)
O2 ⁱⁱⁱ –Mn1–OW1	92.16(6)	P1–O4–Mn1	140.35(9)

Symmetry codes: (i) $x, -y + 3/2, z + 1/2$; (ii) $x + 1/2, y, -z + 3/2$; (iii) $-x + 1, y - 1/2, -z + 3/2$; (iv) $x - 1/2, y, -z + 3/2$; (v) $-x + 1, y + 1/2, -z + 3/2$; (vi) $x, -y + 3/2, z - 1/2$

water molecules in the structure, the formula should be written $(\text{Fe}_{0.54}\text{Mn}_{0.46})(\text{H}_2\text{O})_2(\text{PO}_4)$. The water molecules appear at the ends of an octahedral edge, hence the octahedral structural formula can be written *cis*- $\text{Fe}(\text{O})_4(\text{H}_2\text{O})_2$. To better facilitate packing of such octahedra, the positions of the water molecules would have to become fused to form chains of octahedral structure (Fig. 1) as in laueite (Moore 1965)[19]. In that arrangement, the tetrahedral groups would zigzag up this chain, connecting neighboring octahedral links and cross-linking to other similar chains (Fig. 2).

**Fig. 1** Three-dimensional structure of $(\text{Fe}_{0.54}\text{Mn}_{0.46})(\text{PO}_4)\cdot 2\text{H}_2\text{O}$ viewed along the a axis**Fig. 2** Sheet structure of $(\text{Fe}_{0.54}\text{Mn}_{0.46})(\text{PO}_4)\cdot 2\text{H}_2\text{O}$ along the b axis

The M–O distances in $(\text{Fe}_{0.54}\text{Mn}_{0.46})(\text{PO}_4)\cdot 2\text{H}_2\text{O}$ have values between 1.951(1) and 2.103(2) \AA , exhibiting a strong Jahn–Teller effect. Interatomic angles reveal distortions of the octahedra, varying from $\text{O}(1)^{\text{ii}}\text{–Mn1–OW1} = 82.63(6)^\circ$, $\text{ii} = x + 1/2, y, -z + 3/2$ to $\text{O}(1)^{\text{ii}}\text{–Mn1(1)}\text{–O}(2)^{\text{iii}} = 174.79(6)^\circ$, $\text{iii} = x + 1/2, y, -z + 3/2$. The PO_4 tetrahedron groups can be described as low-distorted tetrahedral with a mean value for the P–O bond distances of 1.535 \AA . The O–P–O angles range from 107.87(9) to 111.03(9)°.

The IR spectrum of $(\text{Fe}_{0.53}\text{Mn}_{0.47})(\text{PO}_4)\cdot 2\text{H}_2\text{O}$ at room temperature in the region between 400 and 4000 cm^{-1} was also determined, complemented by Raman spectroscopy (Figs. 3, 4). The vibrational motions of $(\text{Fe}_{0.53}\text{Mn}_{0.47})(\text{PO}_4)\cdot 2\text{H}_2\text{O}$ may be divided into three classes: The stretching (ν_{OH}) and bending vibrations (δ_{OH}) of water molecules identified, respectively, around 3,422 and 1,638 cm^{-1} , the internal vibrations of $(\text{Fe}_{0.53}\text{Mn}_{0.47})(\text{PO}_4)\cdot 2\text{H}_2\text{O}$ located in the range 1200–400 cm^{-1} , and external optical modes of $(\text{Fe}_{0.53}\text{Mn}_{0.47})(\text{PO}_4)\cdot 2\text{H}_2\text{O}$ situated below 400 cm^{-1} . In the IR spectrum, the strong bands in the region of 1150–950 cm^{-1} are attributed to the P–O stretching vibrations. The bending O–P–O vibrations appear in the region of 450–600 cm^{-1} . The band centred at 668 cm^{-1} can be assigned to $\delta(\text{Mn–O–H})$ by analogy with the observations into $\text{MnAsO}_4 \cdot 1/2\text{H}_2\text{O}$ [20] and $\text{MnPO}_4 \cdot \text{H}_2\text{O}$ [21]. As expected, the vibrational spectra are dominated by the fundamental vibrations of the PO_4^{3-} polyanions which are split in many components due to the correlation effect induced by the coupling with Fe–O and Mn–O units in the structure. In

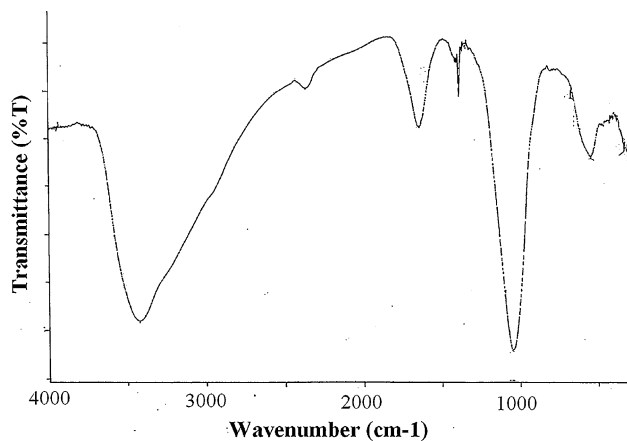


Fig. 3 FTIR spectrum of $(\text{Fe}_{0.54}\text{Mn}_{0.46})(\text{PO}_4)\cdot 2\text{H}_2\text{O}$

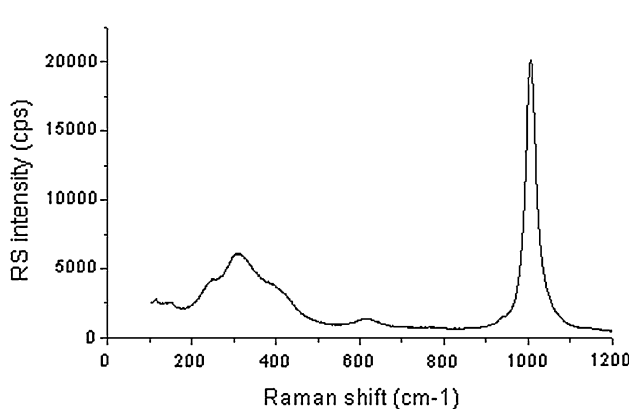


Fig. 4 Raman scattering spectrum of $(\text{Fe}_{0.54}\text{Mn}_{0.46})(\text{PO}_4)\cdot 2\text{H}_2\text{O}$

the region of the internal modes of the phosphate anion (high-wavenumber region), we identify the symmetric and antisymmetric stretching modes, respectively, at 950 and 1085 cm^{-1} . The intensity of antisymmetric mode is greater than that of the symmetric mode one because of the P–O–P bridges. The large band between 570 and 640 cm^{-1} is related to the antisymmetric deformation and the triplet in the range 275–500 cm^{-1} attributed to symmetric deformation mode.

The complex permittivity was measured within the frequency range from 0.1 to 100 kHz with the temperature ranging from 300 to 415 K. In a dielectric under external oscillating field, the answer of the system can be expressed in terms of the complex dielectric permittivity ε^* : $\varepsilon^*(\omega) = \varepsilon'(\omega) + i\varepsilon''(\omega)$; the real part of the complex permittivity of $(\text{Fe}_{0.54}\text{Mn}_{0.46})(\text{PO}_4)\cdot 2\text{H}_2\text{O}$ is used to evaluate its dependence on temperature. Figure 5 shows the plot of ε' at several frequencies. The results show that the dielectric constant of the sample is both frequency dependent and temperature dependent. At low frequency from 300 to 350 K as frequency increases, permittivity increases; from 350 to 415 K as frequency increases, permittivity decreases, resulting in a peak at 350 K. The dielectric constant reaches maximum value of 4939, 4E-12 at the transition point. One explanation is that it is due to the increased conductivity in the sample caused by the presence of Fe^{2+} in $(\text{Fe}_{0.54}\text{Mn}_{0.46})(\text{PO}_4)\cdot 2\text{H}_2\text{O}$. The concentration of Fe^{2+} ions is known to be very sensitive to temperature, and it increases as temperature increases [22]. It is known that the co-existence of Fe^{2+} and Fe^{3+} ions on equivalent crystallographic sites can give rise to an electron-hopping conduction mechanism. Due to the finite hopping (or jump) probability of electrons, this conduction mechanism tends to come into effect only at lower frequencies.

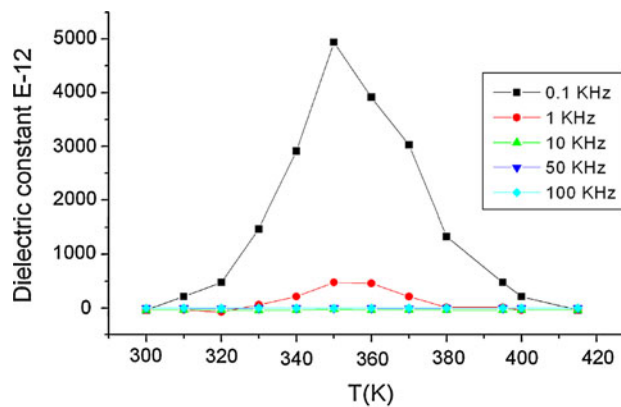


Fig. 5 Dielectric constant of $(\text{Fe}_{0.54}\text{Mn}_{0.46})(\text{PO}_4)\cdot 2\text{H}_2\text{O}$ versus absolute temperature at selected frequencies

Supplementary Information

“Further details of the crystal structure investigations(s) may be obtained in writing from the Fachinformationszentrum Karlsruhe, 76344 Eggenstein-Leopoldshafen, Germany, on quoting the depository number(s) CSD-380288”.

References

1. Marcu IC, Millet JM, Sandulescu I (2001) *Prog Catal* 10:71
2. Davis ME, Lobo RF (1992) *Chem Mater* 4:756
3. Jian-Jiang B, Dong-Wan K, Kug Sun H (2003) *J Eur Ceram Soc* 23:2589
4. Martinelli JR, Sene FF, Gomes L (2000) *J Non Cryst Solid* 263:299
5. Carmen P, Josefina P, Regino SP, Caridad RV, Natalia S (2003) *Chem Mater* 15:3347
6. Lightfoot P, Cheetham AK, Sleight AW (1987) *Inorg Chem* 26:3544
7. Aranda MAG, Attfield JP, Bruque S, Palacio F (1992) *J Mater Chem* 2:501
8. Eventoff W, Martin R (1972) *Am Mineral* 57:45–51
9. Durif A, Averbuch-Pouchot MT (1982) *Acta Crystallogr B* 38:2883
10. Song Y, Zavalij PY, Suzuki M, Whittingham MS (2002) *Inorg Chem* 41(22):5778
11. Rémy P (1971) These de doctorat d'état, faculté des sciences de l'université de Paris
12. Yamada A, Chung SC, Hinokuma K (2001) *J Electrochem Soc* 148(3):A224–A229
13. Yamada A, Hosoya M, Chung SC, Kudo Y, Hinokuma K, Liu KY, Nishi Y (2003) *J Power Sources* 119–121:232–238
14. Padhi AK, Nanjundaswamy KS, Goodenough JB (1997) *J Electrochem Soc* 144:1188
15. Andersson AS, Kalska B, Haggstrom L, Thomas JO (2000) *Solid State Ionics* 130:41
16. North ACT, Phillips DC, Matthews FS (1968) *Acta Cryst* A24:351–359
17. Sheldrick GM (1997) SHELXS97, program for crystal structure solution. University of Göttingen, Germany
18. Sheldrick GM (1997) SHELXL97, program for crystal structure refinement. University of Göttingen, Germany
19. Moore PB (1965) *Am Mineral* 50:1884–1892
20. Aranda MAG, Bruque S, Attfield JP (1991) *Inorg Chem* 30:2043
21. Aranda MAG, Bruque S (1990) *Inorg Chem* 29:1334
22. Singh K, Band SA, Kinge WK (2004) *Ferroelectrics* 306:179